

# DNAJC6 Mutations Associated With Early-Onset Parkinson's Disease

Simone Olgianti, MSc,<sup>1</sup> Marialuisa Quadri, PhD,<sup>1</sup> Mingyan Fang, MSc,<sup>2</sup>  
 Janneke P.M.A. Rood, MD,<sup>3</sup> Jonas A. Saute, MD, PhD,<sup>4</sup>  
 Hsin Fen Chien, MD, PhD,<sup>5</sup> Christian G. Bouwkamp, MSc,<sup>1,6</sup>  
 Josja Graafland, BSc,<sup>1</sup> Michelle Minneboo, BSc,<sup>1</sup> Guido J. Breedveld, BSc,<sup>1</sup>  
 Jianguo Zhang, PhD,<sup>2</sup> The International Parkinsonism Genetics Network,<sup>†</sup>  
 Frans W. Verheijen, PhD,<sup>1</sup> Agnita J.W. Boon, MD, PhD,<sup>3</sup>  
 Anneke J.A. Kievit, MD, PhD,<sup>1</sup> Laura Bannach Jardim, MD, PhD,<sup>4,7</sup>  
 Wim Mandemakers, PhD,<sup>1</sup> Egberto Reis Barbosa, MD, PhD,<sup>5</sup>  
 Carlos R.M. Rieder, MD, PhD,<sup>8</sup> Klaus L. Leenders, MD, PhD,<sup>9</sup>  
 Jun Wang, PhD,<sup>2,10,11,12</sup> and Vincenzo Bonifati, MD, PhD<sup>1</sup>

**Objective:** *DNAJC6* mutations were recently described in two families with autosomal recessive juvenile parkinsonism (onset age < 11), prominent atypical signs, poor or absent response to levodopa, and rapid progression (wheelchair-bound within ~10 years from onset). Here, for the first time, we report *DNAJC6* mutations in early-onset Parkinson's disease (PD).

**Methods:** The *DNAJC6* open reading frame was analyzed in 274 patients with early-onset sporadic or familial PD. Selected variants were followed up by cosegregation, homozygosity mapping, linkage analysis, whole-exome sequencing, and protein studies.

**Results:** We identified two families with different novel homozygous *DNAJC6* mutations segregating with PD. In each family, the *DNAJC6* mutation was flanked by long runs of homozygosity within highest linkage peaks. Exome sequencing did not detect additional pathogenic variants within the linkage regions. In both families, patients showed severely decreased steady-state levels of the auxilin protein in fibroblasts. We also identified a sporadic patient carrying two rare noncoding *DNAJC6* variants possibly effecting RNA splicing. All these cases fulfilled the criteria for a clinical diagnosis of early-onset PD, had symptoms onset in the third-to-fifth decade, and slow disease progression. Response to dopaminergic therapies was prominent, but, in some patients, limited by psychiatric side effects. The phenotype overlaps that of other monogenic forms of early-onset PD.

**Interpretation:** Our findings delineate a novel form of hereditary early-onset PD. Screening of *DNAJC6* is warranted in all patients with early-onset PD compatible with autosomal recessive inheritance. Our data provide further evidence for the involvement of synaptic vesicles endocytosis and trafficking in PD pathogenesis.

ANN NEUROL 2016;79:244–256

View this article online at [wileyonlinelibrary.com](http://wileyonlinelibrary.com). DOI: 10.1002/ana.24553

Received Sep 1, 2015, and in revised form Oct 26, 2015. Accepted for publication Oct 31, 2015.

Address correspondence to Dr Vincenzo Bonifati, Department of Clinical Genetics, Erasmus MC, P.O. Box 2040, 3000 CA Rotterdam, the Netherlands. E-mail: [v.bonifati@erasmusmc.nl](mailto:v.bonifati@erasmusmc.nl); or, Dr Jun Wang, BGI-Shenzhen, Shenzhen 518083, China, E-mail: [wangj@genomics.org.cn](mailto:wangj@genomics.org.cn)

From the <sup>1</sup>Department of Clinical Genetics, Erasmus MC, Rotterdam, the Netherlands; <sup>2</sup>BGI-Shenzhen, Shenzhen, China; <sup>3</sup>Department of Neurology, Erasmus MC, Rotterdam, the Netherlands; <sup>4</sup>Medical Genetics Service, Hospital de Clínicas de Porto Alegre, Porto Alegre, Brazil; <sup>5</sup>Department of Neurology, University of São Paulo, São Paulo, Brazil; <sup>6</sup>Department of Psychiatry, Erasmus MC, Rotterdam, the Netherlands; <sup>7</sup>Department of Internal Medicine, Universidade Federal do Rio Grande do Sul, Porto Alegre, Brazil; <sup>8</sup>Neurology Service, Hospital de Clínicas de Porto Alegre, Porto Alegre, Brazil; <sup>9</sup>Department of Neurology, University Medical Center Groningen, Groningen, the Netherlands; <sup>10</sup>Department of Biology, University of Copenhagen, Copenhagen, Denmark; <sup>11</sup>Princess Al Jawhara Center of Excellence in the Research of Hereditary Disorders, King Abdulaziz University, Jeddah, Saudi Arabia; and <sup>12</sup>Macau University of Science and Technology, Macau, China.

<sup>†</sup>Members of the network are listed in the Supplementary Material.

Additional Supporting Information may be found in the online version of this article.

Parkinson's disease (PD) is a progressive, neurodegenerative disorder manifesting with bradykinesia, resting tremor, muscular rigidity, postural instability, and a good, prolonged response to levodopa and dopaminergic agonists. The ongoing discovery of Mendelian forms of PD provides important clues to understand the disease pathogenesis. Mutations in *Parkin*,<sup>1</sup> *PINK1*,<sup>2</sup> and *DJ-1*<sup>3</sup> cause autosomal recessive forms of early-onset PD (symptoms onset < age 45), which display slow disease progression, absence of atypical signs, and good response to dopaminergic therapies. Different types of autosomal recessive parkinsonisms are caused by mutations in *ATP13A2*,<sup>4</sup> *PLA2G6*,<sup>5</sup> *FBXO7*,<sup>6,7</sup> *DNAJC6*,<sup>8,9</sup> or *SYNJ1*.<sup>10,11</sup> Unlike the previous forms, mutations in these genes cause juvenile-onset (<age 20) parkinsonism with atypical clinical signs and poor or absent response to levodopa.

Mutations in *DNAJC6* [*DnaJ* (*Hsp40*) *Homolog, Subfamily C, Member 6*] were recently described in two consanguineous families with juvenile-onset, atypical parkinsonism, termed PARK19 (MIM 615528). The patients from a Palestinian family carried a homozygous splice-site mutation,<sup>8</sup> whereas those from a Turkish family had a homozygous truncating mutation.<sup>9</sup> In both families, parkinsonism manifested during childhood (<age 11) and the disease progression was very rapid, leading to wheelchair-bound state within ~10 years from onset. The affected family members had poor or absent response to levodopa or additional prominent atypical signs (i.e., mental retardation, seizures, dystonia, and pyramidal signs). Furthermore, a 7-year-old patient carrying a homozygous genomic deletion (including most of the *DNAJC6* exons, but also two neighboring genes) was reported with early-onset obesity, mental retardation, and epilepsy.<sup>12</sup> No clinical signs of parkinsonism were present, but the patient was still very young and his clinical presentation possibly incomplete.

*DNAJC6* encodes the brain-specific isoform of auxilin. Auxilins have a well-established role in the clathrin-mediated endocytosis (CME), the process responsible for the uptake of material into the cells through clathrin-coated vesicles. In neurons, CME is an important mechanism for the formation of new vesicles at the presynaptic terminal and synaptic vesicles recycling.<sup>13</sup>

Previous mutational screenings of *DNAJC6* in PD patients were negative,<sup>8,14,15</sup> but they included only small numbers of patients or tested only a single variant. The role and frequency of *DNAJC6* mutations in PD remained therefore unknown.

Here, by combining direct sequencing, linkage analysis, whole-exome sequencing, and expression studies

of the auxilin protein, we identify novel *DNAJC6* pathogenic mutations in patients with early-onset PD. Our data delineate a novel monogenic form of the disease and have broad implications for understanding the disease pathogenesis, and for improving the diagnostic work-up and the genetic counselling of early-onset PD.

## Subjects and Methods

### Subjects Included in the Study

We studied 274 unrelated probands with PD, including 92 cases with familial PD compatible with autosomal recessive inheritance (mean onset age: 54.65; standard deviation [SD], 12.34; range, 19–84), and 182 patients affected by early-onset sporadic PD (mean onset age: 35.20; SD, 7.98; range, 13–50). The diagnosis of clinically definite PD was made according to the criteria of the UK PD Society Brain Bank<sup>16</sup> (with the exception that a positive family history of PD was not considered an exclusion criterion). The patients were examined and recruited in several movement disorder centers within the International Parkinsonism Genetics Network (members of the network are listed in the Supplementary Material). The patients originated from Italy (n = 147), the Netherlands (n = 78), Brazil (n = 39), Portugal (n = 7), Spain (n = 2), and Turkey (n = 1). Written informed consent was obtained from all the included individuals. This study was approved by appropriate institutional review boards and complied with the legal requirements of the different jurisdictions involved.

### *DNAJC6* Sequencing

Genomic DNA was isolated from peripheral blood or saliva using standard protocols. DNA samples underwent Sanger sequencing of the entire *DNAJC6* coding region and exon-intron boundaries (MIM 608375). Exons and intron-exon boundaries of the *DNAJC6* gene were amplified using polymerase chain reaction (PCR; primers are reported in Supplementary Table 1). Amplification reactions were performed in a total volume of 20  $\mu$ l, containing 1  $\times$  FastStart Taq DNA Polymerase buffer, 200  $\mu$ M of each dNTP, 10  $\mu$ M of forward primer, 10  $\mu$ M of reverse primer, 0.5 units of FastStart Taq DNA Polymerase (Roche, Basel, Switzerland), and 40ng of genomic DNA. PCR conditions: 5 minutes 94  $^{\circ}$ C initial denaturation followed by 30 or 28 cycles of 30 seconds at 94  $^{\circ}$ C; 30 seconds at 60  $^{\circ}$ C; 90 seconds at 72  $^{\circ}$ C, with a final extension for 5 minutes at 72  $^{\circ}$ C.

PCR reactions were purified using 5 units of ExoI and 1 unit of Fast AP (Life Technologies, Carlsbad, CA), 45 minutes at 37  $^{\circ}$ C, 15 minutes at 80  $^{\circ}$ C. Direct sequencing was performed using Big Dye Terminator chemistry (version 3.1; Life Technologies) as recommended by the manufacturer. Dye terminators were removed using SephadexG50 (GE Healthcare, Little Chalfont, UK) and loaded on an ABI 3130XL Genetic Analyzer (Life Technologies). For sequence analysis, the software packages Seqscape v2.6 (Life Technologies) and Sequencing Analysis v5.1 (Life Technologies) were used.

Variants identified were annotated according to the GenBank accession numbers NM\_001256864.1 and NP\_001243793.1, corresponding to the longest protein isoform (auxilin isoform 1).

### Additional Genetic Studies in *DNAJC6* Variant Carriers

Variants were selected for further investigations if they were (1) exonic or with a possible effect on splicing (<100 base pairs [bp] from splice sites), (2) rare in 1000 Genomes (allele frequency < 0.005), and (3) segregating with PD (if additional family members were available). Patients carrying the selected variants were screened for mutations in genes known to cause autosomal recessive, early-onset PD (*parkin*, *PINK1*, and *DJ-1*) by DNA Sanger sequencing and copy number analysis using multiplex ligation-dependent probe amplification (MLPA) kits P051 and P052 (MRC Holland, Amsterdam, the Netherlands). Furthermore, in these patients we sequenced *DNAJC6* 5'UTR (untranslated region), 3'UTR, and promoter regions (1,000 bp upstream of the translation initiation codon of NM\_014787.3), and we performed *DNAJC6* copy number analysis by real-time quantitative PCR (qPCR). Five qPCR assays targeting different exons (2, 5, 10, 15, and 19) of the *DNAJC6* gene were carried out. qPCR reactions contained 200nM of primer, 1 × KAPA SYBR FAST qPCR Master Mix (Kapa Biosystems, Wilmington, MA), and 20ng of genomic DNA. All reactions were performed in triplicates on a Bio-Rad CFX96 Real-Time System. Data were analyzed using CFX Manager Software (v3.0; Bio-Rad Laboratories, Hercules, CA). The assays *SEL1L* and *RBM11* were used as reference targets assuming to detect two chromosomal copies in all the tested samples. PCR conditions: 3 minutes at 94 °C initial denaturation followed by 30 cycles of 5 seconds at 94 °C; and 30 seconds at 60 °C with relative fluorescence units (RFU) data collection. qPCR primers are reported in Supplementary Table 2. All assays were validated by testing linearity over 3 orders of magnitude and by observation of a single peak in RFU data collected during a melting curve as a function of temperature. Intensities were compared to at least two control DNA samples from unrelated or unaffected individuals and two genome reference targets without copy number variations. All copy number values were defined within the normal range for relative quantity values between 0.8 and 1.2.

### Genetic Studies of Families With *DNAJC6* Biallelic Mutations

We identified two familial and one sporadic PD probands carrying biallelic *DNAJC6* variants. To further support the pathogenicity of these variants, all available and consenting affected and unaffected relatives were examined and genomic DNA samples were obtained. The two families with biallelic *DNAJC6* variants were investigated using homozygosity mapping, linkage analysis, and whole-exome sequencing.

### Homozygosity Mapping

DNA samples of the two families underwent genome-wide SNP array genotyping. For the GPS-0313 family, we used Illumina Infinium CytoSNP-850K BeadChip (Illumina,

San Diego, CA; 851,274 single-nucleotide polymorphisms [SNPs] at a median distance of 1.8kb); the DNA samples of the two parents and the three siblings were included. For the PAL-50 family, we employed Illumina HumanOmniExpress BeadChip (Illumina; 730,525 SNPs at a median distance of 2.1 kb); the DNA samples of four siblings were included.

Analysis of homozygosity was performed using Nexus Copy Number, Discovery Edition (v7; BioDiscovery, El Segundo, CA). For the identification of regions of homozygosity shared between affected siblings, the minimum length for homozygous runs was set to 1Mb.

### Linkage Analysis

SNP array data were used to perform parametric multipoint linkage analysis with the software MERLIN (v1.1.2).<sup>17</sup> We assumed an autosomal recessive model, with the following settings: markers allele frequencies set to equal; disease allele frequency set to 0.0001; and penetrances set to 0.0001/0.0001/1.0.

Both the GPS-0313 and PAL-50 families are of white (Caucasian) ethnicity. In both families, the parents of the patients denied consanguinity within at least two previous generations. However, in both families the parents originate from very small villages in peripheral regions of The Netherlands and South Brazil, respectively. Their offspring show several extended (>3Mb) runs of homozygosity, supporting parental consanguinity (Supplementary Table 3). For these reasons, the two families were modeled as consanguineous with the two parents being third cousins. Because the parents of the patients denied consanguinity within at least two previous generations, we considered unlikely a closer consanguineous loop (first or second cousins) and assumed a third-cousins marriage as the closest relatedness. Of note, more distant relatedness between the parents would yield even higher logarithm of odds (LOD) scores at the linkage peak on chromosome 1.

### Whole-Exome Sequencing

We performed whole-exome sequencing of one affected member of each family (GPS-0314 and PAL-54) at BGI Europe. Sequencing was performed using in-solution capturing (Agilent SureSelect Human All Exon V5 50Mb; Agilent Technologies, Santa Clara, CA) and Illumina HiSeq2000, 90 bases paired-end sequencing (Illumina). Reads were aligned to the human reference genome hg19 (build GRCh37.p13) using Burrows-Wheeler Alignment Tool<sup>18</sup> and variants were called using Genome Analysis Toolkit (GATK).<sup>19</sup> Variants were filtered using Cartagenia Bench Lab NGS 4.0 (Agilent Technologies).

Genomic regions of interest were previously determined based on linkage and homozygosity mapping. We selected all the variants that were (1) within the regions of interest, (2) homozygous, (3) nonsynonymous exonic or close to splice sites (<8 bases), and (4) rare in databases (allele frequency lower than 0.01 in 1000 Genomes, Exome Variant Server ESP6500SI-V2, and dbSNP141).

### Additional Linkage and Exome Data Analyses

To exclude the presence of additional novel, likely deleterious variants in the rest of the genome, in both the GPS-0313 and

**TABLE 1. PD Patients and *DNAJC6* Variants Reported in the Study**

Proband ID	Presentation	Affected Relative ID	Age at Onset (yr) <sup>a</sup>	Disease Duration (yr) <sup>a</sup>	<i>DNAJC6</i> Variant	Zygoty	Allele Frequency 1000 Genomes	Allele Frequency ExAC	rs Number
GPS-0313	Familial	GPS-0314	21/29	27/15	c.2779A>G (p.Arg927Gly)	Hom	Absent	Absent	N/A
PAL-50	Familial	PAL-54	42/31	20/15	c.2223A>T (p.Thr741=)	Hom	Absent	Absent	N/A
BR-2652	Sporadic	N/A	33	24	c.2038 + 3A>G c.1468 + 83del	Comp/Het Comp/Het	Absent 0.004010	Absent Absent	N/A rs55883956
COMO-18	Sporadic	N/A	29	21	c.626T>C (p.Leu209Pro)	Het	Absent	Absent	N/A
FI-03	Sporadic	N/A	33	3	c.1855C>T (p.Arg619Cys)	Het	Absent	0.000045	N/A
IT53-RM590	Familial	IT53-RM603	54/58	19/15	c.2517del (p.Phe839Leufs*22)	Het	Absent	Absent	N/A
GPS-60	Sporadic	N/A	27	35	c.397A>T (p.Met133Leu)	Het	0.000200	0.000281	rs61757223
IT59-RM613	Familial	IT59-RM622	65/65	2/11	c.961A>G (p.Ile321Val)	Het	Absent	Absent	N/A
GPS-107B	Sporadic	N/A	42	9	c.1492T>A (p.Cys498Ser)	Het	0.002803	0.001274	rs145329294
SAO-X35	Sporadic	N/A	35	16	c.513G>A (p.Lys171=)	Het	0.001200	0.000305	rs148204207
COMO-05	Sporadic	N/A	24	35	c.801-84C>A	Het	0.000400	Absent	rs52001060
PV-16	Familial	N/A	64	6	c.995 + 86C>T	Het	Absent	Absent	N/A
TH-20	Sporadic	N/A	30	2	c.2108-21A>G	Het	Absent	0.000017	N/A
TOR-6A	Sporadic	N/A	44	26	c.2634 + 37A>G	Het	Absent	Absent	N/A

Biallelic mutations and mutations predicted to be deleterious are bolded.

<sup>a</sup>For familial cases, the column reports data of proband/affected relative. Hom = homozygous; Het = heterozygous; Comp/Het = compound heterozygous; N/A = data not available.

PAL-50 families we also performed genome-wide linkage analysis under autosomal recessive inheritance using the parameters set as above, but assuming no parental relatedness.

Regions with positive values of LOD scores were then inspected using whole-exome sequencing data (obtained in the GPS-0314 and PAL-54 patients). We selected all the variants that were: (1) within linkage regions; (2) nonsynonymous exonic or close to splice sites (<8 bases); (3) absent from public databases (1000 Genomes, Exome Variant Server ESP6500SI-V2, dbSNP141, and Exome Aggregation Consortium); and (4) homozygous or double heterozygous (heterozygous variants located in genes with multiple heterozygous variants fulfilling criteria 1, 2, and 3).

### **In Silico and Structural Analysis**

The effect of the missense variants identified in the study was investigated using five different protein damage prediction software: Sorting Intolerant From Tolerant (SIFT),<sup>20</sup> PolyPhen-2,<sup>21</sup> likelihood ratio test (LRT),<sup>22</sup> MutationTaster,<sup>23</sup> and MutationAssessor.<sup>24</sup> Moreover, variants with a possible effect on splicing were tested using five splicing prediction tools (SpliceSite-Finder-like, MaxEntScan,<sup>25</sup> NNSPLICE,<sup>26</sup> GeneSplicer,<sup>27</sup> and Human Splicing Finder<sup>28</sup>) integrated in Alamut Visual v4.2 (Interactive Biosoftware, Rouen, France).

The effect of the *DNAJC6* missense mutation (p.Arg927-Gly) was investigated using publicly available X-ray crystallographic structures of the bovine auxilin J domain. The sequences of the auxilin protein homologs in *Homo sapiens* and *Bos Taurus* were aligned using the software T-Coffee.<sup>29</sup> The homologs were completely identical in the domain under study (J domain). Crystallographic structures of the auxilin J domain, and the complex between auxilin J domain and the ATPase domain of Hsc70 (AMPPNP form) were retrieved from the Protein Data Bank (PDB ID 1NZ6 and 2QWR).<sup>30,31</sup> A modified structure with the mutant amino acid was generated with the UCSF Chimera package (v1.10.1). Chimera is developed by the Resource for Biocomputing, Visualization, and Informatics at the University of California, San Francisco (supported by NIGMS P41-GM103311).<sup>32</sup> Molecular graphics and analyses were performed with the Pymol Molecular Graphics System v1.5.0.5 (Schrodinger, New York, NY).

### **Protein Expression Analysis**

To investigate further the pathogenicity of the *DNAJC6* variants identified, we analyzed the expression of the auxilin protein in patient-derived fibroblasts. Primary fibroblasts were obtained from skin biopsies of both the Dutch patients (GPS-0313 and GPS-0314) and one of the two Brazilian patients with novel homozygous *DNAJC6* mutations (PAL-54), one unaffected relative of the Dutch family, who was a heterozygous mutation carrier (GPS-0315), and four unrelated unaffected control donors. The expression of auxilin was studied in protein extracts from fibroblasts using Western blotting.

Fibroblast cell lines were expanded in growth medium (Dulbecco's modified Eagle's medium, 15% fetal calf serum, penicillin, and streptavidin), and at 90% confluence lysed in

radioimmunoprecipitation assay lysis buffer (150mM NaCl, 1.0% IGEPAL CA-630, 0.5% sodium deoxycholate, 0.1% sodium dodecyl sulphate, and 50 mM of Tris, pH 8.0.) containing protease inhibitor Complete (Roche). Lysates were cleared by spinning 10,000g for 10 minutes. For Western blotting, proteins were precipitated using the TCA protein precipitation protocol,<sup>33</sup> separated on 4% to 15% Criterion TGX precast gels (Bio-Rad Laboratories), and transferred to nitrocellulose using the Trans-Blot Turbo Transfer System (Bio-Rad Laboratories). Blots were blocked using 5% Protifar (Nutricia, Amsterdam, the Netherlands) in phosphate-buffered saline (PBS), 0.1% (v/v) TWEEN 20 (Sigma-Aldrich, St. Louis, MO). Primary antibodies used were: rabbit anti-auxilin (1:1,000; a gift from Dr Pietro De Camilli, Yale University, New Haven, CT of note, this antibody is validated for the detection of endogenous auxilin in Western blotting)<sup>34</sup>; rabbit anti-gamma-tubulin (1:2,000; Sigma-Aldrich T5192); mouse anti-vinculin (Clone V284; 1:5000; Santa Cruz Biotechnology, Dallas, TX). After washing in PBS, 0.1% (v/v) TWEEN 20, blots were incubated with fluorescently conjugated goat anti-mouse (IRDye 800) and goat anti-rabbit (IRDye 680) secondary antibodies (LI-COR Biosciences, Lincoln, NE). After washing in PBS, 0.1% (v/v) TWEEN 20, the blots were imaged and analyzed using an Odyssey Imaging system (LI-COR).

Images were analyzed by removing the median background from the total intensity of each band. Auxilin intensities were divided by intensities of the loading control vinculin and normalized using the sum of all data points in each replicate.<sup>35</sup> Four independent biological replicates of each individual were analyzed by signal quantification of multiple Western blots (12 technical replicates in total). The technical replicates belonging to the same biological replicate were averaged and used for the statistical analysis. We performed one-way analysis of variance (ANOVA) using eight groups, one for each subject (four unrelated healthy donors, GPS-0313, GPS-0314, GPS-0315, and PAL-54). Post-hoc test between the control subjects and the remaining individuals were conducted using pair-wise *t* tests and correcting for multiple comparisons (Bonferroni's correction). Statistical analyses were conducted in R (v3.2.1; R Foundation for Statistical Computing, Vienna, Austria).

## **Results**

### ***DNAJC6* Genetic Studies**

The results of the *DNAJC6* sequencing analysis in the 274 PD probands are displayed in Table 1 and Figure 2C. We identified 14 samples with a total of 15 exonic or possible-splicing variants passing our filtering criteria. To exclude the possibility that any of these variants was in linkage disequilibrium with other variants in the gene, we also screened the entire *DNAJC6* 5'UTR, 3'UTR, and part of the promoter in these 14 samples, but no additional pathogenic variants were detected. Moreover, qPCR experiments could not detect any copy number variants in *DNAJC6*. Also, none of these 14 samples carried pathogenic variants in *parkin*, *PINK1*, and *DJ-1*.

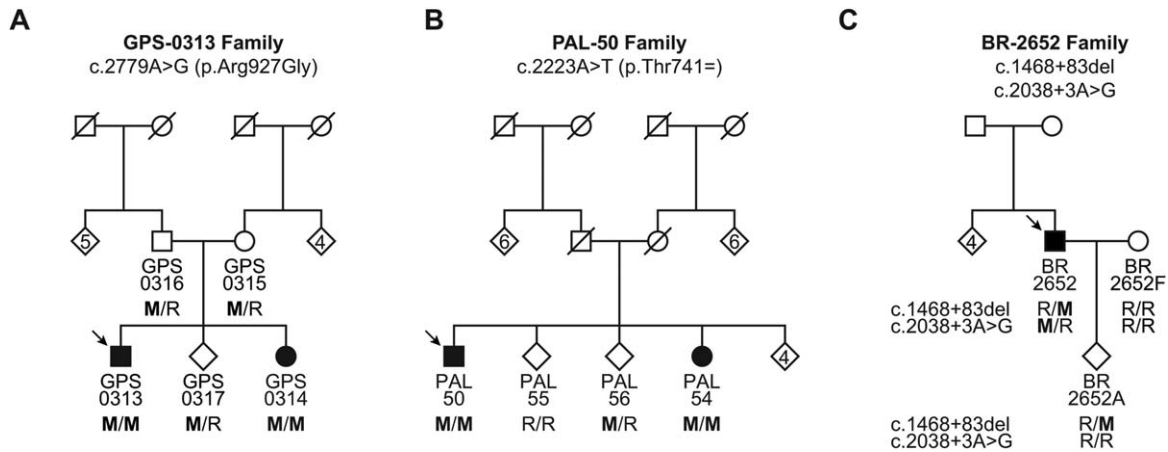


**FIGURE 1:** Pedigrees of the PD patients with biallelic *DNAJC6* mutations. The genotypes of the available family members are reported. To protect subjects' privacy, the sex of some individuals has been disguised. Black symbols denote individuals affected by early-onset PD. PD = Parkinson's disease; M = mutation; R = reference (normal sequence).

Three probands carried *DNAJC6* homozygous or double heterozygous variants (Fig 1). GPS-0313 and PAL-50, two patients with familial early-onset PD, carried novel homozygous mutations in *DNAJC6*, whereas BR-2652, a patient with early-onset sporadic PD, carried two heterozygous variants with possible effect on splicing. The clinical features of these patients are reported in Table 2.

### Family GPS-0313

A novel homozygous *DNAJC6* c.2779A>G variant (predicted protein effect: p.Arg927Gly) was present in GPS-0313, a Dutch proband with early-onset, familial PD compatible with autosomal recessive inheritance (Fig 2A). Sanger sequencing of his affected sister (GPS-0314) revealed the same homozygous mutation, whereas his parents and one healthy sibling were heterozygous mutation carriers (Fig 1A).

Genome-wide linkage analysis revealed a single, nearly significant peak on chromosome 1 (maximum LOD: 3.07), including the *DNAJC6* locus. In this region, homozygosity mapping showed a 10.7-Mb run of homozygosity (from rs6660751 to rs10789400) present in both affected siblings, but absent from the unaffected family members (Fig 3A,D). Exome sequencing in one of the affected siblings, GPS-0314, achieved an average coverage of 132 $\times$ , with 91% of the target regions covered at least 10 $\times$  (Supplementary Table 4). According to our filtering criteria, the p.Arg927Gly was the only likely pathogenic variant within the linkage region. Also, this variant was absent from all the databases tested, including the Exome Aggregation Consortium (ExAC; 121,412 alleles),<sup>36</sup> and was predicted to be pathogenic by all the prediction software (Supplementary Table 5). Notably,

the variant was also absent in the Genome of the Netherlands (GoNL) database.<sup>37</sup>

These two patients developed the first motor symptoms, bradykinesia and tremor, during the third decade of life. In one of them, GPS-0313, parkinsonism signs developed after 6 months of neuroleptic treatment, prescribed for psychotic disturbances since the age of 21. Over the years, the motor disorder progressed slowly. Their magnetic resonance imaging (MRI) and F-18 fluorodeoxyglucose/positron emission tomography (<sup>18</sup>F-FDG PET) were unremarkable, whereas <sup>18</sup>F-DOPA PET imaging revealed nigrostriatal abnormalities compatible with PD. Supplementary Videos 1 and 2 display these patients after 27 and 16 years of disease evolution. GPS-0313 had more severe parkinsonism and was wheelchair-bound, whereas, remarkably, his sister had very little postural instability and relatively preserved gait. Of note, both patients responded well to dopaminergic therapies, but the dosages had to be limited to control psychiatric side effects.

### Family PAL-50

A different, novel *DNAJC6* homozygous variant, c.2223A>T (p.Thr741=; Fig 2A), was present in PAL-50, a Brazilian proband with early-onset, familial PD compatible with autosomal recessive inheritance. This variant is located 5 bases before the end of exon 15. Sanger sequencing confirmed the mutation in homozygous state in the affected sister (PAL-54), whereas two unaffected siblings were heterozygous (PAL-56) or non-carriers (PAL-55; Fig 1B). Also in this family, linkage analysis identified a single, nearly significant peak on chromosome 1 (LOD score: 3.18), corresponding to a 16.1-Mb homozygous run (from rs3118027 to rs6672527; Fig 3B,D). Exome sequencing in PAL-54

TABLE 2. Clinical Features in PD Patients With Biallelic DNAJC6 Mutations

Patient Code	GPS-0313	GPS-0314	PAL-50	PAL-54	BR-2652
Sex	Male	Female	Male	Female	Male
Age at last examination (yr)	48	44	62	46	57
Onset age (yr)	~21	29	42	31	33
Disease duration (yr)	~27	15	20	15	24
Symptoms at onset	Motor slowness <sup>a</sup> hand tremors <sup>a</sup>	Hand tremor	Motor slowness	Hand tremor	Hand tremor
Asymmetric onset	-	+	+	+	+
Signs at examination					
Hoehn-Yahr stage	5	3	3	3	4
Bradykinesia	+	+	+	+	+
Rest tremor	-	+	+	+	+
Rigidity	+	+	+	+	+
Postural instability	+	+	+	+	+
Levodopa response	+	+	+	+	+
Motor fluctuations	-	-	+	+	+
Levodopa-induced dyskinesias	-	-	+	+	+
Levodopa-induced hallucinations	+	+	+	-	-
Pyramidal signs	-	-	-	-	-
Cerebellar signs	-	-	-	-	-
Autonomic signs	-	-	-	-	-
Cognitive decline	-	-	+	-	-
Seizures	-	-	-	-	-
Brain MRI	Normal	Normal	Normal	Normal	Normal
Brain <sup>18</sup> F-Dopa PET	Abnormal <sup>b</sup>	Abnormal <sup>b</sup>	N/P	N/P	N/P
Brain FDG PET	Normal	Normal	N/P	N/P	N/P
Surgical therapies	None	None	None	STN-DBS	pallidotomy

+ = present; - = absent; N/P = not performed.

<sup>a</sup>Parkinsonism symptoms initially emerged after treatment with neuroleptics.

<sup>b</sup>Severe striatal uptake deficit, particularly at putamen level, as seen in PD.

PD = Parkinson's disease; MRI = magnetic resonance imaging; PET = positron emission tomography; FDG = F-18 fluorodeoxyglucose; STN-DBS = treated with deep-brain stimulation of the subthalamic nuclei.

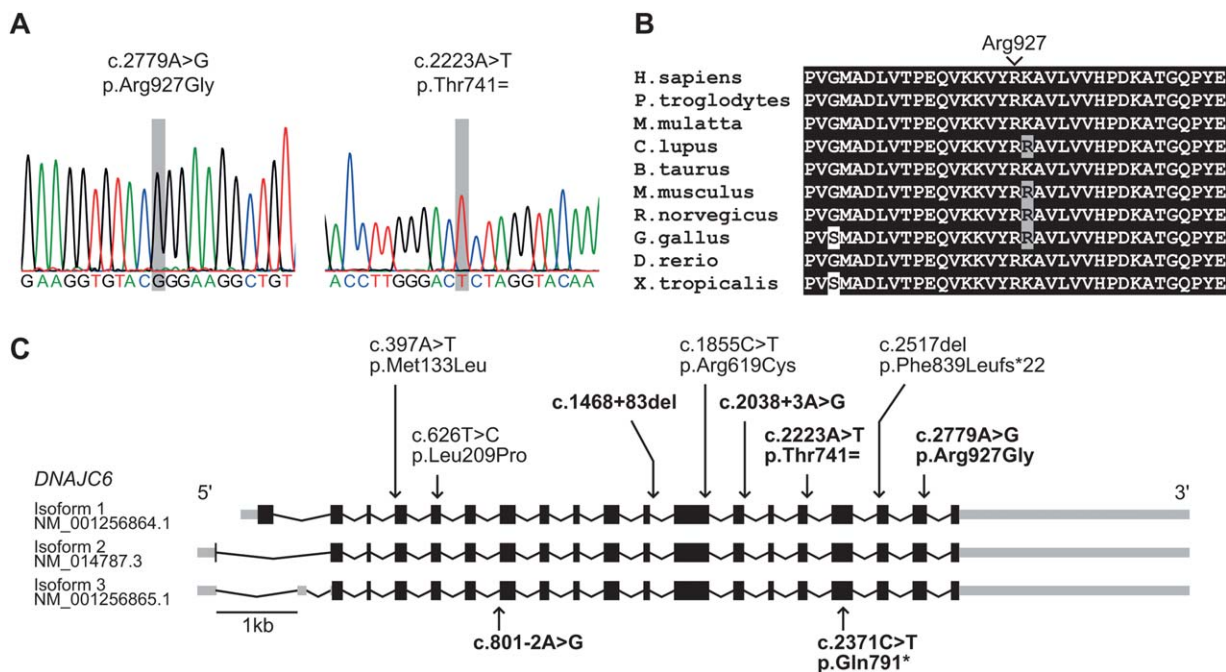


**FIGURE 2: *DNAJC6* mutations.** (A) Electropherograms of the two *DNAJC6* homozygous mutations. (B) Alignment of the auxilin protein homologs in different species (protein accession numbers are reported in Supplementary Table 8). Protein homologs in different species were aligned using the software T-Coffee.<sup>29</sup> The arginine at position 927 is also indicated. (C) Schematic representation of the *DNAJC6* transcripts with the mutations previously identified in the two PARK19 families (bottom) and the novel mutations identified here in patients with early-onset PD (top). Mutations detected in homozygous or compound heterozygous state are bolded. PD = Parkinson's disease.

achieved an average coverage of  $141 \times$  with 91% of the target regions covered at least  $10 \times$  (Supplementary Table 4). Within this linkage region, exome sequencing revealed two additional homozygous variants besides the *DNAJC6* c.2223A>T: a c.589A>G (p.Arg197Gly) in *LITDI* (NM\_001164835.1) with an allele frequency of 0.003 in 1000 Genomes and ExAC and a novel c.2065G>A (p.Gly689ser) in *HOOK1* (NM\_015888.4). Both variants were excluded from further investigations because predicted to be benign by all the protein damage prediction tools, and because conservation analysis showed that species other than humans carry the mutated amino acids (Supplementary Table 6). On the contrary, the *DNAJC6* c.2223A>T variant was absent from all the available databases, including the ExAC, and three of the five prediction software tools suggested a splicing effect: the introduction of an aberrant splicing acceptor site 1 base after the constitutive donor site, at position 2227 + 1 (Supplementary Table 7). These two patients developed PD symptoms at the age of 42 and 31, respectively. Their clinical course was typical for PD, including good response to levodopa and severe motor complications (wearing off and dyskinesia). Because of these, PAL-54 also underwent bilateral subthalamic nucleus DBS, with marked improvement. Supplementary Videos 3 and 4 display the patients at the ages of 62 and 46 years.

**Proband BR-2652**

Two *DNAJC6* heterozygous variants, a novel c.2038 + 3A>G and a c.1468 + 83del with allele frequency of 0.004 in 1000 Genomes, were present in BR-2652, a sporadic Brazilian patient with early-onset PD (Fig 1C). Genotyping of available relatives was consistent with the patient being compound heterozygous. Four of five splicing prediction software suggested that the c.2038 + 3A>G variant may cause loss of the splicing donor site at position 2038, whereas the same analysis for the c.1468 + 83del did not suggest an effect on splicing (Supplementary Table 7). This proband developed PD at the age of 33, with right-hand tremor. The parkinsonism was responsive to levodopa and displayed a prolonged course. He also received left-side pallidotomy in 2006 and right-side pallidotomy in 2010. Supplementary Video 5 displays the patient at the age of 44, after 11 years of disease.

**Additional Linkage and Exome Data Analyses**

Our linkage analysis assuming no parental relatedness identified positive LOD scores in 33 genomic regions (total: 671Mb; maximum LOD: 0.23) in the GPS-0313 family and 32 regions (total: 383Mb; maximum LOD: 0.24) in the PAL-50 family. The analysis of the whole exome sequencing data revealed the *DNAJC6*

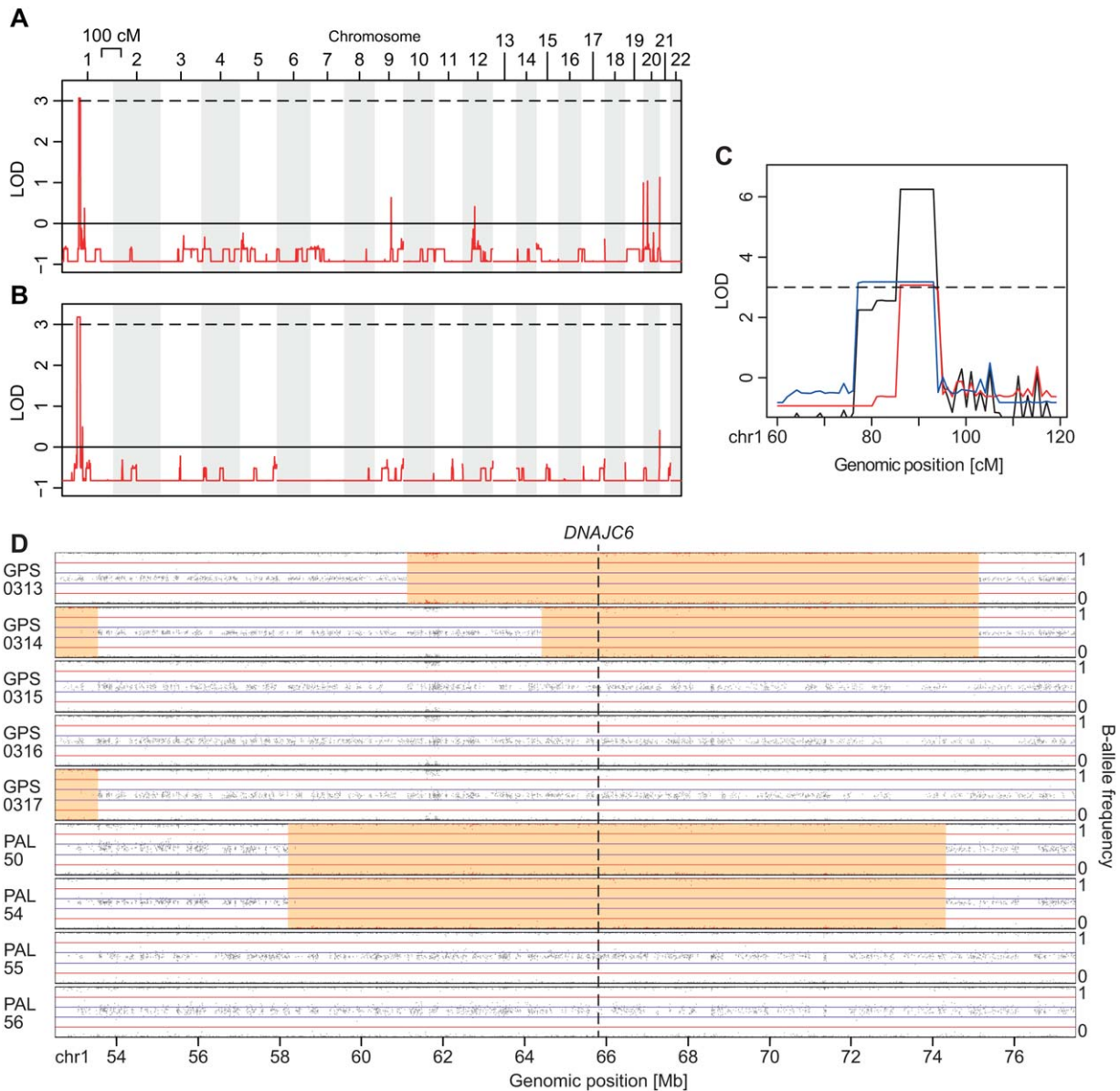


**FIGURE 3: Genome-wide linkage analysis and homozygosity mapping.** Genome-wide linkage analysis of the GPS-0313 (A) and PAL-50 (B) families. Values of LOD score (red lines) were calculated for all the autosomes applying a grid of 1cM. (C) Linkage analysis of the chromosome 1 locus. Red line, GPS-0313 family; blue line, PAL-50 family; black line, cumulative LOD score. Dashed lines mark the LOD score threshold of 3.0. (D) Homozygosity mapping of GPS-0313 and PAL-50 families showing the overlapping regions of homozygosity on chromosome 1. For each available sample of the two families, and for each probe in the region, probe B-allele frequency (vertical axis) is represented as a function of its genomic position (horizontal axis). Dashed line indicates the position of the *DNAJC6* locus; red probes and orange areas indicate regions of homozygosity longer than 1Mb. LOD = logarithm of odds.

c.2779A>G (p.Arg927Gly) as the only variant surpassing our filtering criteria in GPS-0314.

In PAL-54, this analysis revealed only two variants, which were already identified by our homozygosity-based strategy, within the chromosome 1 linkage peak: the *DNAJC6* c.2223A>T and the *HOOK1* c.2065G>A (p.Gly689ser). Additional novel variants were not detected. Further inspection of the exome data revealed a heterozygous variant in the glucocerebrosidase gene (*GBA*; NM\_000157.3: c.1088T>C, p.Leu363Pro) in

PAL-54, which was present also in PAL-50. *GBA* variants were not found in the exome data of GPS-0314. Heterozygous *GBA* variants are known to be risk factors for the development of PD. However, the p.Leu363Pro variant has never been reported in patients with this disease.

#### Expression and Structural Studies of the Auxilin Protein

The results of our protein expression studies showed that, in primary fibroblasts, the steady-state levels of

**TABLE 3. Statistical Analysis of *DNAJC6* Expression in Subject-Derived Fibroblasts**

	GPS-0313	GPS-0314	GPS-0315	PAL-54
Control 1	<b><math>6.6 \times 10^{-06}</math></b>	<b><math>1.3 \times 10^{-05}</math></b>	0.02702	<b><math>1.7 \times 10^{-04}</math></b>
Control 2	<b><math>3.0 \times 10^{-04}</math></b>	<b><math>5.8 \times 10^{-04}</math></b>	0.40799	<b>0.00715</b>
Control 3	<b><math>2.3 \times 10^{-05}</math></b>	<b><math>4.5 \times 10^{-05}</math></b>	0.07662	<b><math>6.0 \times 10^{-04}</math></b>
Control 4	<b><math>1.3 \times 10^{-06}</math></b>	<b><math>2.5 \times 10^{-06}</math></b>	<b>0.00600</b>	<b><math>3.1 \times 10^{-05}</math></b>

The table displays the *p* values for pair-wise *t* test comparisons between controls and subjects with *DNAJC6* mutations. *p* values are not corrected for multiple testing. Values surpassing the Bonferroni-corrected threshold ( $p < 0.0125$ ) are bolded.

auxilin are markedly and significantly lower in patients with homozygous *DNAJC6* mutations than in control subjects (ANOVA  $p = 1.08 \times 10^{-06}$ ; Table 3; Fig 4A,B). The unaffected heterozygous mutation carrier (GPS-0315) had auxilin levels intermediate between those of controls and patients.

Furthermore, our in silico structural studies showed that the Arginine at position p.927 (replaced by Glycine in the patients of the Dutch family) is located in the J domain, which is a known crucial functional domain of

auxilin, and it is facing the interacting partner, Hsc70. The mutation has a drastic steric effect and reduces the charge potential of a positively charged patch at the protein surface, a region possibly involved in the interaction with Hsc70, or with other molecular partners (Fig 4C,D).

**Discussion**

Our study reveals a novel role for *DNAJC6* mutations in early-onset PD. Two of the ninety-two probands (2.2%)

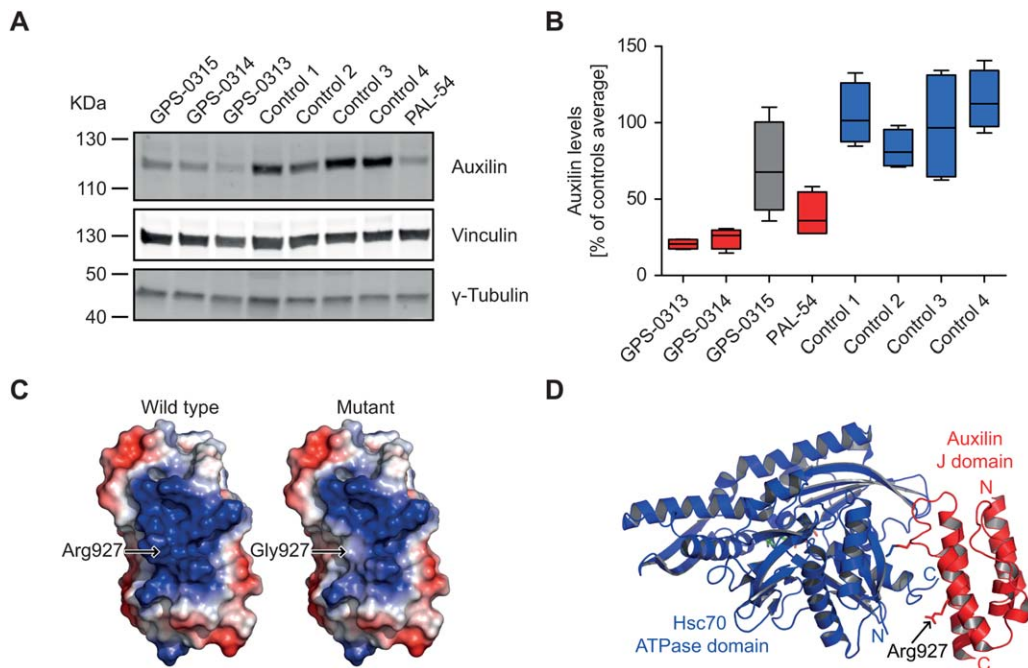


**FIGURE 4: Protein analyses. (A)** Auxilin expression in human fibroblasts; a representative Western blot is shown; vinculin and  $\gamma$ -tubulin are included as loading controls. **(B)** Quantitative analysis of auxilin levels in patients' fibroblasts, expressed as percentage of the average expression in 4 unrelated control individuals. All data are from four biological replicates. The plots of the patients with *DNAJC6* homozygous mutations are in red; the heterozygous carrier of the Dutch missense mutation (GPS-0315) is in gray; the control subjects are in blue. **(C)** Crystal structure of the bovine auxilin J domain with visualization of the electrostatic potential surface for the wild-type (left) and mutant (right) proteins (PDB accession no.: 1NZ6). The replacement of the Arginine-927 with a Glycine modifies a large positively charged patch on the protein surface, with drastic steric and electrostatic consequences. The more positively charged regions are displayed in blue, whereas negatively charged regions are displayed in red; the position of the residue homolog to the human Arginine-927 is indicated. **(D)** Crystal structure of the bovine auxilin J domain complexed with the Hsc70 ATPase domain and ATP analog (PDB accession no.: 2QWR). The residue homolog to the human Arginine-927 is located in the auxilin domain (red) that interacts with Hsc70 (blue). The Arginine-927 points toward Hsc70, suggesting a possible involvement in the interaction between the two proteins.

with familial PD compatible with autosomal recessive inheritance carried novel homozygous mutations.

Several lines of evidence support the contention that the two homozygous variants identified are disease causing. First, each of these variants is located within the highest, and nearly significant, linkage peak obtained in the respective family (Fig 3A–C) and also supported by the results of the homozygosity mapping. Second, within these linkage regions, exome sequencing revealed no evidence of disease-causing variants in genes other than *DNAJC6*. Moreover, novel pathogenic variants were not found by exome sequencing in any other genomic loci detected in the two families under an autosomal recessive mode of inheritance, without assuming parental consanguinity. Third, both variants are absent from all the available databases (more than 120,000 alleles). Fourth, the two variants are predicted to be deleterious by our in silico analyses. Last, the steady-state levels of auxilin are markedly and significantly decreased in fibroblasts of patients from both families (Fig 4A,B), providing compelling experimental evidence for the pathogenicity of the *DNAJC6* homozygous mutations. Of note, these results also delineate a loss-of-function mechanism for these mutations, in keeping with the recessive disease inheritance in these families.

The c.2779A>G (p.Arg927Gly) mutation is classified as disease causing by all the prediction tools, it replaces an amino acid that has been highly conserved in evolution (Fig 2B), and is located within the J domain. Moreover, the mutation appears to cause a substantial modification of the biochemical properties of the domain (Fig 4A,B). This could affect the protein stability, or binding to Hsc70, or both, and would be in keeping with the observed decreased levels of auxilin protein in patients' fibroblasts. The synonymous c.2223A>T is predicted to affect splicing by the majority of the prediction software tested. To investigate the effect of the c.2223A>T, we also undertook *DNAJC6* mRNA expression analysis in fibroblasts, but the expression levels in control subjects were unreliable (data not shown). This is in keeping with the known fact that *DNAJC6* messenger RNA expression is essentially brain specific and very low in any other tissues (EST profile in NCBI UniGene: Hs.647643).<sup>8,38</sup> Furthermore, we cannot exclude the possibility that this synonymous variant is in linkage disequilibrium with another causative variant located in introns or other noncoding regulatory elements of *DNAJC6*, which were not detectable by our screening.

We also identified a sporadic patient with early-onset PD with two rare, compound heterozygous *DNAJC6* variants. Because of its novelty and the results of the splicing prediction software, the c.2038 + 3A>G

variant appear to be likely deleterious. Instead, the c.1468 + 83del is only moderately rare in databases, and the evidence of its splicing effect is less compelling. Despite being unable to conclusively prove their pathogenicity, the coexistence in the same patient of these two rare variants in trans is intriguing and suggests a pathogenic nature. Furthermore, as said before, we cannot exclude the possibility that one or both of these variants are in linkage disequilibrium with other causative variants located in introns or other noncoding regulatory elements, which were not detectable by the methods used here. Unfortunately, fibroblasts from this patient were unavailable to perform protein expression studies.

We also detected 11 patients with rare heterozygous variants in *DNAJC6*, but sequencing and gene dosage assays did not reveal additional mutations in these samples. Interestingly, at least four of the heterozygous variants identified (p.Phe839Leufs\*22, p.Leu209Pro, p.Met133Leu, and p.Arg619Cys) are either novel or extremely rare in databases and are predicted to have a deleterious effect for the protein function (Supplementary Table 5), which is dramatic in the case of the frameshift variant (p.Phe839Leufs\*22). These variants might be a coincidental finding. However, we cannot exclude that additional variants *in trans* were missed because they are outside the sequenced regions or undetectable by our assays. Another hypothesis is that single heterozygous variants in *DNAJC6* act as risk factors for PD. Similar hypotheses have been proposed for single heterozygous variants in other genes causing autosomal recessive PD.<sup>39</sup> It will be interesting to test this hypothesis for *DNAJC6* in future studies.

From the clinical standpoint, our patients with homozygous *DNAJC6* mutations have a very different phenotype than the PARK19 patients reported earlier. The Palestinian and Turkish patients developed motor symptoms during childhood (before < 11 years old) and were all wheelchair-bound or bedridden within ~10 years from onset. Furthermore, they displayed atypical clinical signs, such as mental retardation, seizures, and dystonia, or they had poor or absent response to levodopa.<sup>8,9</sup> On the contrary, the patients identified in our study developed parkinsonism in their third to fifth decade of life, experienced a much slower disease progression, and they all responded well to dopaminergic therapies, including DBS in 1 case. These clinical features are compatible with the diagnosis of early-onset PD and overlap the phenotype of other monogenic forms of PD caused by *parkin*, *PINK1*, or *DJ-1* mutations. It is possible that the phenotypic variability is owing to the fact that the novel mutations identified here might allow some residual activity to the auxilin protein. In other

words, our data suggest a possible genotype-phenotype correlation in patients with *DNAJC6* mutations, with complete loss-of-function variants causing the juvenile, atypical form (PARK19), whereas milder mutations (described in our study) cause early-onset PD. The observation of severely reduced, but detectable, residual levels of auxilin protein in the fibroblasts of our patients fits very well with this hypothesis.

The established role of auxilin in the CME is crucial for neurons that need CME for the formation of new vesicles at the presynaptic terminal and synaptic vesicles recycling.<sup>13</sup> Together with their molecular partner, Hsc70, auxilins are essential to complete the last step of the CME, the uncoating of the vesicles after their separation from the plasma membrane.<sup>13,40</sup>

Our findings add to a growing body of evidence for the involvement of synaptic vesicles recycling in PD. First, recessive mutations in *SYNJ1*, encoding another close molecular partner of auxilin, cause early-onset parkinsonism (PARK20).<sup>10,11</sup> The knockout mice models of *DNAJC6* and *SYNJ1* display similar severe neurological phenotypes, with defective synaptic vesicle recycling, and clathrin-coated vesicle accumulation.<sup>41,42</sup> Second, common variants in *GAK* (encoding auxilin-2, a different ubiquitously expressed form of auxilin) have been identified by genome-wide association studies as a risk factor for late-onset idiopathic PD.<sup>43,44</sup> Last, the protein products of other genes causing Mendelian PD have been linked to the recycling of synaptic vesicles. The LRRK2 and parkin protein interact with endophilin-A<sup>45,46</sup>; the VPS35 protein is part of the retromer complex that recycles membrane-associated protein to the trans-Golgi network<sup>47</sup>; and  $\alpha$ -synuclein has been implicated in several ways to vesicles recycling and release.<sup>48,49</sup>

In conclusion, the identification of early-onset PD patients with *DNAJC6* mutations changes the current view of *DNAJC6*, from being the cause of a rare and atypical juvenile parkinsonism, to be the fourth gene involved in autosomal recessive, early-onset PD. Screening of *DNAJC6* is therefore warranted in all patients with early-onset PD compatible with autosomal recessive inheritance, with broad implications for the diagnostic workup and genetic counseling of patients. Our data provide further support for disturbed synaptic vesicle endocytosis and trafficking in the pathogenesis of PD.

## Acknowledgment

This work was supported by research grants from the Stichting ParkinsonFonds (The Netherlands; to A.J.W.B. and V.B.) and by the Beijing Genomics Institute (BGI).

We thank all the patients involved in the study and their families. We also thank Dr Pietro De Camilli for kindly providing the anti-auxilin antibody.

## Author Contributions

S.O., M.Q., M.F., J.G., G.J.B., and J.Z. acquired, analyzed, and interpreted the genetic data. J.P.M.A.R., J.A.S., H.F.C., C.G.B., A.J.W.B., A.J.A.K., L.B.J., E.R.B., C.R.M.R., K.L.L., and members of the International Parkinsonism Genetics Network acquired, analyzed, and interpreted the clinical data. M.M., F.W.V., and W.M. acquired, analyzed, and interpreted the protein expression data. J.W. and V.B. conceived and designed the study and interpreted the clinical and laboratory data. S.O., M.Q., J.W., and V.B. drafted the manuscript. All the authors critically revised the article for important intellectual content and approved the version to be published. S.O., M.Q., and M.F. contributed equally to this work, as first authors. J.W. and V.B. contributed equally to this work, as senior authors.

## Potential Conflicts of Interest

Nothing to report.

## References

1. Kitada T, Asakawa S, Hattori N, et al. Mutations in the parkin gene cause autosomal recessive juvenile parkinsonism. *Nature* 1998;392:605–608.
2. Valente EM, Abou-Sleiman PM, Caputo V, et al. Hereditary early-onset Parkinson's disease caused by mutations in PINK1. *Science* 2004;304:1158–1160.
3. Bonifati V, Rizzo P, van Baren MJ, et al. Mutations in the DJ-1 gene associated with autosomal recessive early-onset parkinsonism. *Science* 2003;299:256–259.
4. Ramirez A, Heimbach A, Grundemann J, et al. Hereditary parkinsonism with dementia is caused by mutations in ATP13A2, encoding a lysosomal type 5 P-type ATPase. *Nat Genet* 2006;38:1184–1191.
5. Paisan-Ruiz C, Bhatia KP, Li A, et al. Characterization of PLA2G6 as a locus for dystonia-parkinsonism. *Ann Neurol* 2009;65:19–23.
6. Shojaaee S, Sina F, Banihosseini SS, et al. Genome-wide linkage analysis of a Parkinsonian-pyramidal syndrome pedigree by 500 K SNP arrays. *Am J Hum Genet* 2008;82:1375–1384.
7. Di Fonzo A, Dekker MC, Montagna P, et al. FBXO7 mutations cause autosomal recessive, early-onset parkinsonian-pyramidal syndrome. *Neurology* 2009;72:240–245.
8. Edvardson S, Cinnamon Y, Ta-Shma A, et al. A deleterious mutation in *DNAJC6* encoding the neuronal-specific clathrin-uncoating co-chaperone auxilin, is associated with juvenile parkinsonism. *PLoS One* 2012;7:e36458.
9. Koroglu C, Baysal L, Cetinkaya M, Karasoy H, Tolun A. *DNAJC6* is responsible for juvenile parkinsonism with phenotypic variability. *Parkinsonism Relat Disord* 2013;19:320–324.
10. Quadri M, Fang M, Picillo M, et al. Mutation in the *SYNJ1* gene associated with autosomal recessive, early-onset Parkinsonism. *Hum Mutat* 2013;34:1208–1215.

11. Krebs CE, Karkheiran S, Powell JC, et al. The Sac1 domain of SYNJ1 identified mutated in a family with early-onset progressive parkinsonism with generalized seizures. *Hum Mutat* 2013;34:1200–1207.
12. Vauthier V, Jaillard S, Journel H, Dubourg C, Jockers R, Dam J. Homozygous deletion of an 80kb region comprising part of DNAJC6 and LEPR genes on chromosome 1P31.3 is associated with early onset obesity, mental retardation and epilepsy. *Mol Genet Metab* 2012;106:345–350.
13. Kononenko NL, Haucke V. Molecular mechanisms of presynaptic membrane retrieval and synaptic vesicle reformation. *Neuron* 2015;85:484–496.
14. Foo JN, Liang H, Tan LC, et al. DNAJ mutations are rare in Chinese Parkinson's disease patients and controls. *Neurobiol Aging* 2014;35:935.e1–2.
15. Jesus S, Gomez-Garre P, Carrillo F, et al. Analysis of c.801-2A>G mutation in the DNAJC6 gene in Parkinson's disease in southern Spain. *Parkinsonism Relat Disord* 2014;20:248–249.
16. Hughes AJ, Daniel SE, Kilford L, Lees AJ. Accuracy of clinical diagnosis of idiopathic Parkinson's disease: a clinico-pathological study of 100 cases. *J Neurol Neurosurg Psychiatry* 1992;55:181–184.
17. Abecasis GR, Cherny SS, Cookson WO, Cardon LR. Merlin—rapid analysis of dense genetic maps using sparse gene flow trees. *Nat Genet* 2002;30:97–101.
18. Li H, Durbin R. Fast and accurate short read alignment with Burrows-Wheeler transform. *Bioinformatics* 2009;25:1754–1760.
19. McKenna A, Hanna M, Banks E, et al. The Genome Analysis Toolkit: a MapReduce framework for analyzing next-generation DNA sequencing data. *Genome Res* 2010;20:1297–1303.
20. Kumar P, Henikoff S, Ng PC. Predicting the effects of coding non-synonymous variants on protein function using the SIFT algorithm. *Nat Protoc* 2009;4:1073–1081.
21. Adzhubei IA, Schmidt S, Peshkin L, et al. A method and server for predicting damaging missense mutations. *Nat Methods* 2010;7:248–249.
22. Chun S, Fay JC. Identification of deleterious mutations within three human genomes. *Genome Res* 2009;19:1553–1561.
23. Schwarz JM, Rodelsperger C, Schuelke M, Seelow D. MutationTaster evaluates disease-causing potential of sequence alterations. *Nat Methods* 2010;7:575–576.
24. Reva B, Antipin Y, Sander C. Predicting the functional impact of protein mutations: application to cancer genomics. *Nucleic Acids Res* 2011;39:e118.
25. Yeo G, Burge CB. Maximum entropy modeling of short sequence motifs with applications to RNA splicing signals. *J Comput Biol* 2004;11:377–394.
26. Reese MG, Eeckman FH, Kulp D, Haussler D. Improved splice site detection in Genie. *J Comput Biol* 1997;4:311–323.
27. Pertea M, Lin X, Salzberg SL. GeneSplicer: a new computational method for splice site prediction. *Nucleic Acids Res* 2001;29:1185–1190.
28. Desmet FO, Hamroun D, Lalonde M, et al. Human Splicing Finder: an online bioinformatics tool to predict splicing signals. *Nucleic Acids Res* 2009;37:e67.
29. Notredame C, Higgins DG, Heringa J. T-Coffee: a novel method for fast and accurate multiple sequence alignment. *J Mol Biol* 2000;302:205–217.
30. Jiang J, Taylor AB, Prasad K, et al. Structure-function analysis of the auxilin J-domain reveals an extended Hsc70 interaction interface. *Biochemistry* 2003;42:5748–5753.
31. Jiang J, Maes EG, Taylor AB, et al. Structural basis of J cochaperone binding and regulation of Hsp70. *Mol Cell* 2007;28:422–433.
32. Pettersen EF, Goddard TD, Huang CC, et al. UCSF Chimera—a visualization system for exploratory research and analysis. *J Comput Chem* 2004;25:1605–1612.
33. Link AJ, LaBaer J. Trichloroacetic acid (TCA) precipitation of proteins. *Cold Spring Harb Protoc* 2011;2011:993–994.
34. Milosevic I, Giovedi S, Lou X, et al. Recruitment of endophilin to clathrin-coated pit necks is required for efficient vesicle uncoating after fission. *Neuron* 2011;72:587–601.
35. Degasperis A, Birtwistle MR, Volinsky N, et al. Evaluating strategies to normalise biological replicates of Western blot data. *PLoS One* 2014;9:e87293.
36. Exome Aggregation Consortium (ExAC), Cambridge, MA. Available at: <http://exac.broadinstitute.org>. Accessed August 31, 2015.
37. Genome of the Netherlands Consortium. Whole-genome sequence variation, population structure and demographic history of the Dutch population. *Nat Genet* 2014;46:818–825.
38. Ishikawa K, Nagase T, Nakajima D, et al. Prediction of the coding sequences of unidentified human genes. VIII. 78 new cDNA clones from brain which code for large proteins in vitro. *DNA Res* 1997;4:307–313.
39. Klein C, Lohmann-Hedrich K, Rogaeva E, Schlossmacher MG, Lang AE. Deciphering the role of heterozygous mutations in genes associated with parkinsonism. *Lancet Neurol* 2007;6:652–662.
40. Ungewickell E, Ungewickell H, Holstein SE, et al. Role of auxilin in uncoating clathrin-coated vesicles. *Nature* 1995;378:632–635.
41. Yim YI, Sun T, Wu LG, et al. Endocytosis and clathrin-uncoating defects at synapses of auxilin knockout mice. *Proc Natl Acad Sci U S A* 2010;107:4412–4417.
42. Cremona O, Di Paolo G, Wenk MR, et al. Essential role of phosphoinositide metabolism in synaptic vesicle recycling. *Cell* 1999;99:179–188.
43. Pankratz N, Wilk JB, Latourelle JC, et al. Genomewide association study for susceptibility genes contributing to familial Parkinson disease. *Hum Genet* 2009;124:593–605.
44. Nalls MA, Pankratz N, Lill CM, et al. Large-scale meta-analysis of genome-wide association data identifies six new risk loci for Parkinson's disease. *Nat Genet* 2014;46:989–993.
45. Matta S, Van Kolen K, da Cunha R, et al. LRRK2 controls an EndoA phosphorylation cycle in synaptic endocytosis. *Neuron* 2012;75:1008–1021.
46. Trempe JF, Chen CX, Grenier K, et al. SH3 domains from a subset of BAR proteins define a Ubl-binding domain and implicate parkin in synaptic ubiquitination. *Mol Cell* 2009;36:1034–1047.
47. Bonifacino JS, Hurley JH. Retromer. *Curr Opin Cell Biol* 2008;20:427–436.
48. Nemani VM, Lu W, Berge V, et al. Increased expression of alpha-synuclein reduces neurotransmitter release by inhibiting synaptic vesicle re-clustering after endocytosis. *Neuron* 2010;65:66–79.
49. Burre J, Sharma M, Tsetsenis T, Buchman V, Etherton MR, Sudhof TC. Alpha-synuclein promotes SNARE-complex assembly in vivo and in vitro. *Science* 2010;329:1663–1667.